A Shock-Tube, Laser-Schlieren Study of the Dissociation of 1,1,1-Trifluoroethane: An Intrinsic Non-RRKM Process

J. H. Kiefer,* C. Katopodis, S. Santhanam, N. K. Srinivasan, and R. S. Tranter

Department of Chemical Engineering, University of Illinois at Chicago, Chicago, Illinois 60607

Received: August 4, 2003; In Final Form: January 12, 2004

We report a shock-tube, laser-schlieren investigation of the molecular dissociation of the title trifluoroethane, $CF_3CH_3 \rightarrow CH_2CF_2 + HF$, over very high temperatures, 1600−2400 K, and a wide range of sub-atmospheric pressures, 15−550 Torr. The density gradients are well fit by a simple two-reaction mechanism and accurate dissociation rates obtained. The results are compared with a k_∞ calculated from a G3 TS for this molecular elimination, which is a superb fit to the available lower-T data and a reliable extrapolation of k_∞ to high temperatures. The derived rate constants show a very deep falloff from this extrapolation but surprisingly little variation with pressure. This peculiarity is so severe that RRKM calculations dramatically fail to account for the behavior. The dissociation seems to be a clear example of an intrinsic non-RRKM process (nonstatistical dissociation). This conclusion is strongly supported by the observation of double vibrational relaxation at both dissociating and nondissociating temperatures, an unambiguous demonstration of slow IVR. Using a simple model with division into two groups of states, the deep falloff is found to be consistent with a rate-controlling slow IVR, not with low collision efficiency. The model suggests an IVR rate of $\sim 10^8$ s^{-1} for dissociation energies.

Introduction

In a shock-tube study of the thermal dissociation of 1,1,1-trifluoroethane

$$CF_3CH_3 \rightarrow CH_2CF_2 + HF \qquad (A)$$

we have found serious problems modeling the rates with RRKM theory. This reaction appears to offer the most unambiguous example of an "intrinsic" non-RRKM unimolecular process, i.e., one resulting from random excitation,[1] that has yet been seen.

Nonstatistical unimolecular reaction has long been anticipated by theorists,[1,2] has been demonstrated in many model systems,[3] and observed in chemical activation,[2,4,5] but experimental illustration of truly intrinsic non-RRKM behavior has proved to be quite elusive. There are a few extant claims, but almost all have problems. Of the more convincing examples there is the isomerization of *trans*-stilbene,[6] a recent shock-tube study of dissociation in H_2O_2,[7] and a large reported difference between predicted and extrapolated k_∞ in methyl recombination,[8] again at high temperatures. Although some indications of non-RRKM behavior are thus beginning to appear, this statistical theory has proven to be remarkably successful over a truly broad range of application.[2] Our own very high-temperature results showing severe falloff in large molecules have always been in excellent accord with the theory.[9−11]

Some have expressed surprise at the wide applicability of RRKM theory, but it is really not so remarkable. To have an observable deviation, it is necessary for the reaction rate to become comparable to or greater than some IVR rate in the molecule,[1] so that IVR is at least partially rate controlling. We now know that such intramolecular relaxation processes are extremely fast, with measured rate constants from 10^8 to 10^{13}/s.[12] Obviously, it would be very difficult to observe thermal rates this fast, and in any case, with reasonable pressures most unimolecular reactions will be very deep into falloff well before they reach such rates. Then collisional activation would be rate controlling and any effect of slow IVR would again be obscured. This last seems to have been a difficulty with the aforementioned study of H_2O_2 dissociation.[7] In general, it is necessary to stay well away from the low-pressure limit, so large molecules are clearly the best choice.

Fortunately, it is not necessary for $k(T)$ to exceed 10^8/s for observable deviations to occur; it is enough that some of the $k(E)$ involved are this large. Nonetheless, to find significant deviations the rate will certainly have to be quite rapid, and this usually means high temperatures. There is little hope of finding such behavior when rates are little over 1/s, as in the much studied[13−15] isomerization of CH_3NC.

The present study is able to uncover non-RRKM behavior in the title reaction because the combination of shock-tube and laser-schlieren (LS) measurements accesses temperatures where a theoretical/extrapolated k_∞ reaches 10^6-10^8/s. That the relatively slow IVR rate or rates still needed for a clearly discernible nonstatistical process do exist here, at least at low energies, is unambiguously confirmed by the observation of a double vibrational relaxation in some very low-pressure experiments.

Experimental Section

The shock tube used in the experiments has a 4 ft long driver section of 4 in. i.d. connected to a 10 ft driven section of 2.5 in. i.d., an arrangement whose details have been very fully described.[16] Details of the laser-schlieren diagnostics have also been given before.[17] The data acquisition system for the LS experiment has recently been upgraded, giving improved sensitivity and resolution, but again this has been fully described elsewhere.[10,11] In addition to the improved hardware, the control

* Corresponding author. E-mail: kiefer@uic.edu.

10.1021/jp036282h CCC: $27.50
Published on Web 03/05/2004

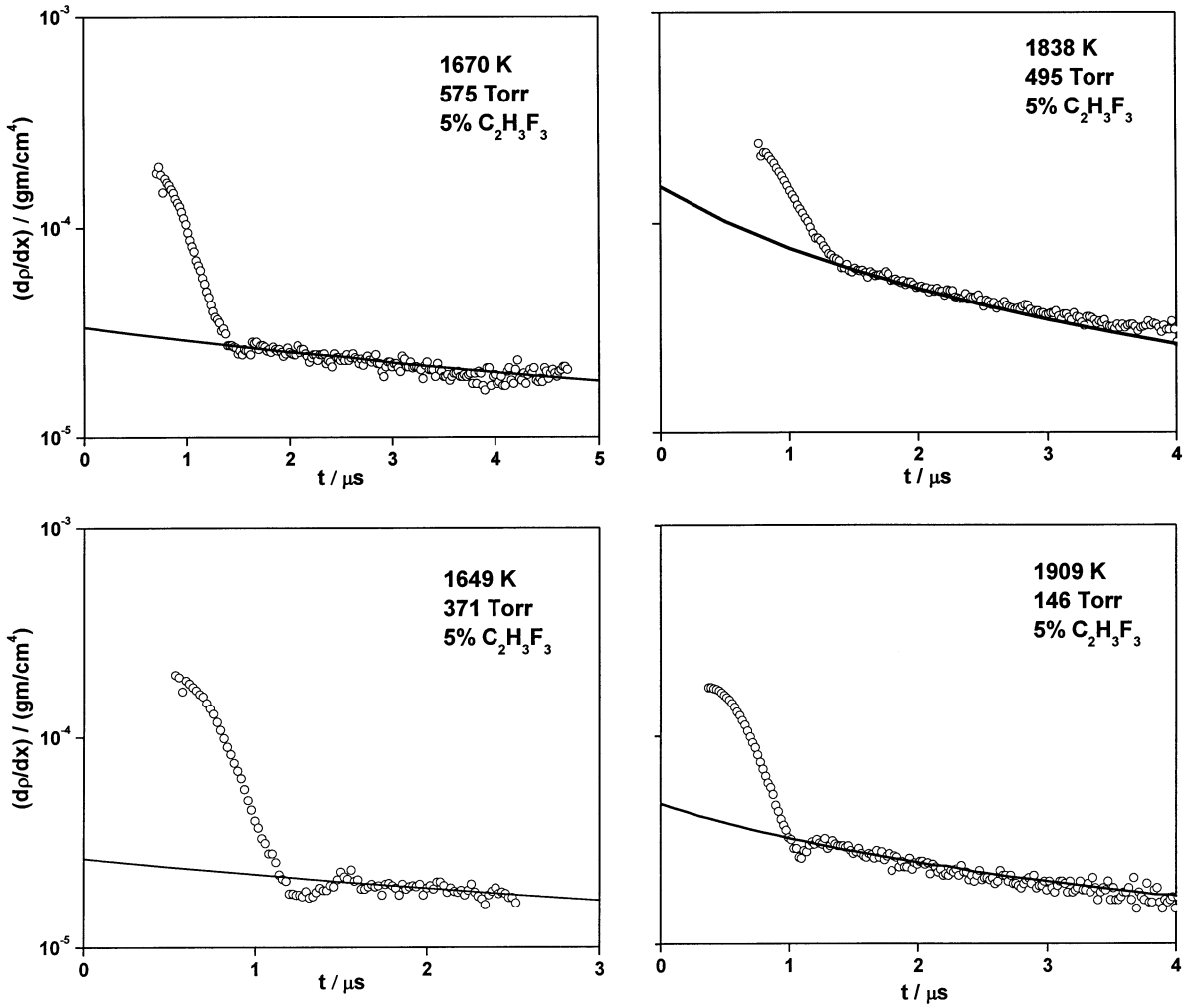

Figure 1. Example dissociation density gradients in 2% CH_3CF_3−Kr (○) and modeling of these (solid lines) for moderate to high pressures. Here temperatures and pressures are all vibrationally relaxed, chemically frozen, ideal post-incident shock values, values used at the start of the modeling shown as a solid line (see text). The initial steep drop in each is a consequence of shock-front diffraction/refraction, as is the small dip after this evident in three of these examples. This last occurs often in LS experiments, but only for pressures above about 100 Torr.

and analysis software have also been updated. Among other features, the software now determines the chemically frozen, but vibrationally equilibrated, shock parameters and also calculates the Blythe and Blackman corrections[18] used in the analysis for vibrational relaxation times. As before,[16] velocities were set by interpolation of four intervals calculated from measured times centered about the LS beam. On the basis of extensive experience, the uncertainty in velocity is estimated as ±0.2%, corresponding to a temperature error of < ±0.5%, here ∼ ±10 K.

Trifluoroethane was obtained from Lancaster (99%), and krypton was Spectra Gases excimer grade. Mixtures were prepared manometrically in a 50-L glass vessel and stirred for 2 h using a Teflon-coated magnetic stirrer. Mixtures of 2%, 5%, and 10% CF_3CH_3 in Kr were used, with uncertainties in composition of less than ±1%.

To produce the very weak shocks necessary for observation of relaxation, incubation, and falloff in these high molecular weight mixtures, a slow flow of driver gas was achieved by introducing various converging/diverging nozzles of different throat diameters at the diaphragm. The experiments all used Mylar diaphragms of 0.003, 0.004, and 0.005 in. thickness, burst spontaneously with helium. Molar refractivities used in the calculation for density gradient from measured angular deflection were 10.696 for trifluoroethane and 6.367 for Kr.[19] These were taken as constant throughout the decomposition.

Unless otherwise noted, thermodynamic functions for CF_3CH_3 ($\Delta_f H°_{298}$, C_p, and $H°(T) - H°_{298}$) and for other species encountered herein, were obtained from the NIST compilations of S. E. Stein[20] and the NIST computational chemistry database.[21]

Results

Dissociation. Example LS density gradients showing dissociation in CF_3CH_3 are presented in Figures 1 and 2. The two groups differ in that the latter set has much lower pressures and there is then a small but significant incubation delay which must be recognized for accurate location of the beginning of reaction in the modeling. The origin of the delays indicated in these figures is discussed in the following section. The computed gradients also shown in these figures all used the two-step mechanism

$$CF_3CH_3 \rightarrow CH_2CF_2 + HF \quad \Delta H°_{298} = 31.8 \text{ kcal/mol} \quad \text{(A)}$$

$$CH_2CF_2 \rightarrow CHCF + HF \quad \Delta H°_{298} = 42.9 \text{ kcal/mol} \quad \text{(B)}$$

There is good reason to believe that this simple scheme is

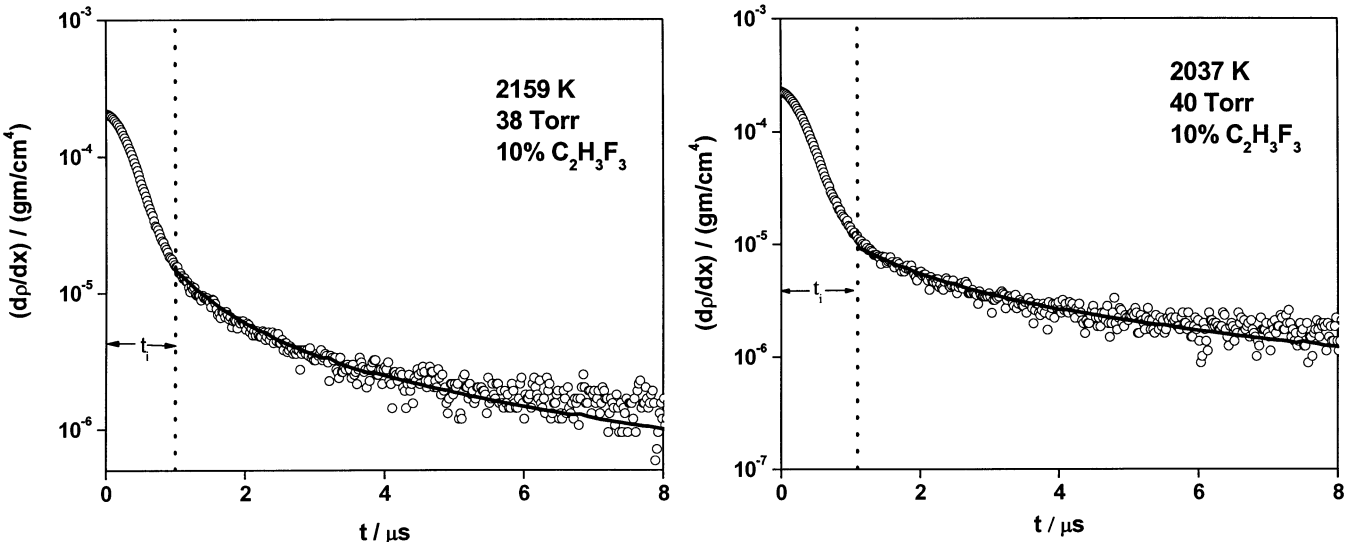

Figure 2. Example density gradients caused by dissociation in 2% CH_3CF_3−Kr (○), and modeling of these (solid lines), for low pressures. Here temperatures and pressures are again vibrationally relaxed, chemically frozen, ideal incident shock values. At such low pressures the dissociation is preceded by a short but significant incubation delay, t_i, (see text), as indicated by the vertical dotted lines.

perfectly adequate in the present situation. Other possible dissociation paths have very much higher energies and likely barriers. For example, C−H fission, $CF_3CH_3 \rightarrow \bullet CH_2CF_3 + H$, has $\Delta H^\circ_{298} = 107$ kcal/mol and that for C−C fission is 101 kcal/mol. The diradical route, $CF_3CH_3 \rightarrow CH_3F + :CF_2$, has $\Delta H^\circ_{298} = 74$ kcal/mol, but its barrier must be much higher than this, whereas the ΔH°_{298} for the HF elimination (reaction A) is just 31.8 kcal/mol and the barrier for this molecular process is just 71.7 kcal/mol (see below). Also, inasmuch as the dissociation observed herein is deep into falloff throughout, it is most unlikely that higher-energy channels will contribute.[22]

As expected, and as illustrated in Figures 1 and 2, the modeling is quite successful with just reactions (A) and (B). The contribution of reaction (B) is significant only at the higher temperatures, where it is responsible for much of the gradient after about 4−5 μs. The rate constant expression for this used throughout the modeling was log k(B) s^{-1} = 13.1−80 kcal/mol/2.303RT. Although the late-time gradient is thus sensitive to this, it is unlikely to influence the choice of rate for (A), as this strongly dominates the early gradients, and these were emphasized in the extraction of rate constants.

Anticipating the possibility of a complex P- and T-dependence of the rates for reaction (A), these were obtained by a process of iteration. First, rates for this reaction were estimated by an extrapolation of the gradient profiles to our best estimate of $t = 0$,[10,11,18] or to the end of the incubation delay, during which this of course is the only reaction. The derived estimates were then plotted (simple Arrhenius is good enough over a small range) and the expressions derived for each pressure were used in a full modeling that took account of temperature variation in the experiment. Minor adjustments were then made to produce an optimum fit. In only a very few instances was it necessary to correct and repeat the modeling, because the initial estimated rates for $t = 0$ are quite close to the final optimum values. Nonetheless, each separate experiment created its own individual rate constant taken from the extrapolated value at $t = 0$ using the final modeling to inform the extrapolation. The derived rates are shown in Figure 3. Here the only useful way to estimate probable error is through intercomparison. In other words, the probable error in these results is best indicated by the scatter.

Figure 3 has the derived rate constants, an extrapolated/theoretical k_∞, and some RRKM calculations discussed below.

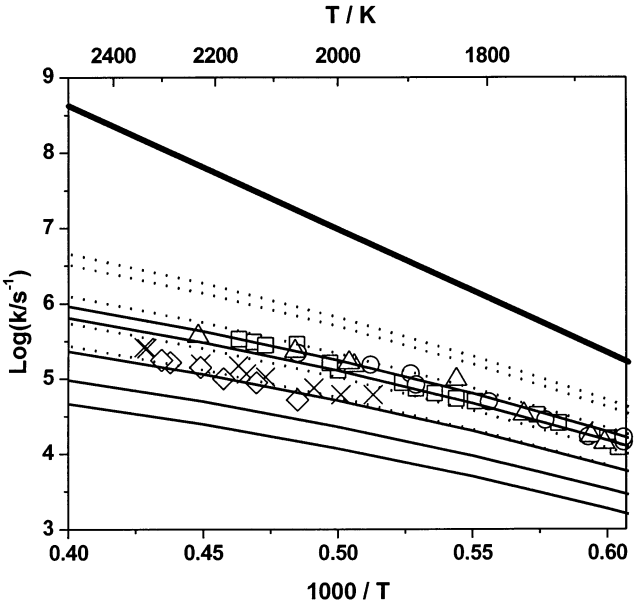

Figure 3. Rate constants for reaction (A), HF loss, in 2% CH_3CF_3−Kr; [Δ] 550 Torr, 5% CH_3CF_3−Kr [○] 350 Torr, [□] 100 Torr; 10% CH_3CF_3−Kr [×] 35 Torr; 5% CH_3CF_3−Kr [◇] 15 Torr. In each instance the pressures cited are mean values for experiments covering a small range of pressures. The lower sets of lines show two RRKM calculations: A "high" collision efficiency with $\langle \Delta E \rangle_{down} = 1100$ cm^{-1} (···) and a "low" efficiency with $\langle \Delta E \rangle_{down} = 350$ cm^{-1} (—). For both calculations the lines show results for the cited mean pressures in ascending order. The heavy, steep line at the top displays the k_∞ taken from the TST/G3 calculation described in the text.

Here the k_∞ is taken from a conventional transition-state-theory (TST) calculation using G3[23] calculated properties of both the TS and the molecule, calculations performed by D. C. Fang and L. B. Harding. These calculated properties are given with the RRKM parameters in Table 1. They were used for all RRKM calculations without modification. The existing literature rates for reaction (A) are certainly close to, if not at, the high-pressure limit, and these are compared with the TST calculation in Figure 4. As seen, this calculation is in superb agreement with the majority of the data. The experiments of Cadman and coworkers[26] would appear to be in error, but the present study

TABLE 1: RRKM Model[a] for Reaction (A), $C_2H_3F_3 \rightarrow C_2H_2F_2 + HF$

Molecular vibrational frequencies (cm^{-1}) and degeneracies	3330(2), 3246(1), 1627(2), 1600(1), 1429(1), 1414(2), 1094(2), 907(1), 645(1), 584(2), 391(2), 249(1)[b]
Transition state vibrational frequencies (cm^{-1}) and degeneracies	3428(1), 3332(1), 1875(1), 1710(1), 1617(1), 1552(1), 1452(1), 1128(1), 1023(1), 971(1), 796(1), 656(1), 524(1), 507(1), 428(1), 298(1), 260(1)
Moments of inertia ($\times 10^{-40}$ g cm^2)	
Molecular adiabatic:	550.28, 550.28
Transition state adiabatic:	641.34, 653.87
Molecular active:	515.65
Transition state active:	514.47
Reaction path degeneracy	9
$E_o(=\Delta H^0_0)$ (kcal/mol)	71.7
$\langle\Delta E\rangle_{down}$ (cm^{-1})	350, 1100 and finally 1000 (see text)
Number of Morse oscillators	3
L−J collision parameters	
Collision diameters[c] (angstroms)	CF_3CH_3: 4.9589, Kr: 3.6100
ϵ/k potential well depth (K)	CF_3CH_3: 0.3872E+3, Kr: 0.1900E+3
For slow IVR model, $k_2 = 8 \times 10^7$ s^{-1}	

[a] The RRKM code used here is a widely used and well-tested version of the scheme presented by Gilbert et al.[37] [b] The torsion is treated as a vibration throughout. Here the barrier to internal rotation is 1137 cm^{-1}, and restricted rotor calculations[38] confirm the accuracy of this approximation to the highest temperatures. Anharmonic effects of internal rotation in $\rho(E)$ are included by the addition of Morse oscillators, following the suggestion of J. Troe.[39] [c] Collision frequencies were Lennard-Jones values from $Z_{L-J} = N_A\sigma_{A-M}^2(8RT/\pi\mu_{A-M})^{1/2}\Omega(2,2)^*$. The collision integrals $\Omega(2,2)^*$ were taken from the empirical expressions of Troe.[40]

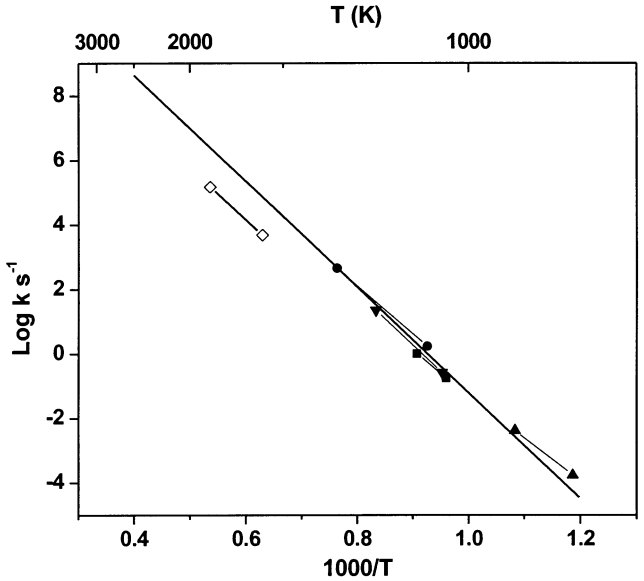

Figure 4. Literature rate data on the trifluoroethane dissociation, reaction (A): ●−●, ref 25, for $P = 3.2-4.53$ atm; ▼−▼, ref 27, 2.53 bar; ◇−◇, ref 26, 1.07−1.2 bar; ■−■, ref 28, (P unknown); ▲−▲, ref 24, 1.0 atm. The thick solid line shows the result of the G3/TST calculation of k_∞ described in the text. Here, this rate is remarkably close to Arrhenius with $\log k_\infty(s^{-1}) = 15.2-75.033$(kcal/mol)/2.303$RT$ ± 0.005% over 830−2500 K.

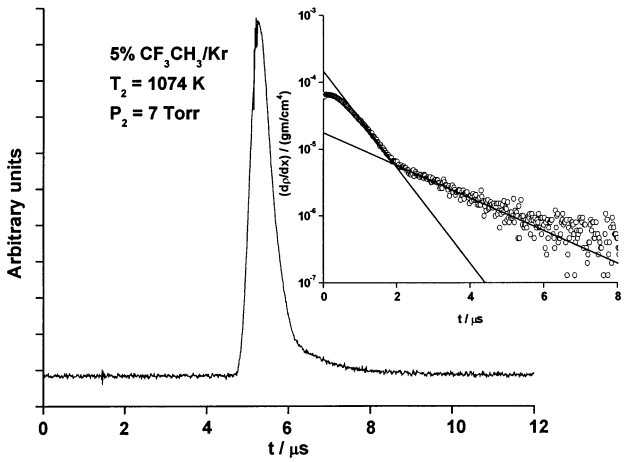

Figure 5. Vibrational relaxation of trifluoroethane in a very low-P experiment whose temperature is much too low for discernible dissociation. The large picture shows the "raw" unprocessed recording of voltage from LS beam deflection. This picture exhibits the usual initial diffraction/refraction "spike" which is followed here by clearly separated "fast" and "slow" sequential exponential decays showing a double relaxation. The inset has a semilog plot of gradient from the same signal, together with solid-line fits to the two exponential stages seen in the gradient decay. The first portion of this plot retains some residual diffraction/refraction signal from the shock front.

ultimately suggests that this may not be so; they may actually be reduced by some pressure-independent IVR falloff (see below).

Before considering the RRKM calculations presented in Figure 3, the qualitative features of the results should be recognized. One is first struck by the very severe falloff; the measured rates lie between more than 1 to nearly 3 orders of magnitude below k_∞ over the 1600−2300 K temperature range, yet show a rather weak variation with pressure. Some difficulty in producing a RRKM fit to these data may thus be anticipated, and this problem is amply borne out by the attempts shown in the figure. Here we show two calculations, one with a small $\langle\Delta E\rangle_{down} = 350$ cm^{-1}, which brings the calculations near the high-pressure results, but leaves the low-pressure calculations far too low, and a second with a "large" $\langle\Delta E\rangle_{down} = 1100$ cm^{-1} that is now close to the low-P data but much too high for the higher pressures. We have found no way to reconcile this large discrepancy and therefore conclude that this is a particularly severe example of non-RRKM behavior. The discrepancy seems far too large for minor faults in the RRKM calculation or in the data to disturb this conclusion.

Relaxation. The strongly nonstatistical behavior in the dissociation rates noted above implies, or better requires, there be some slow IVR rate in this molecule. In fact, the presence of such a slow rate is quite unambiguously established by our observations of vibrational relaxation in trifluoroethane.

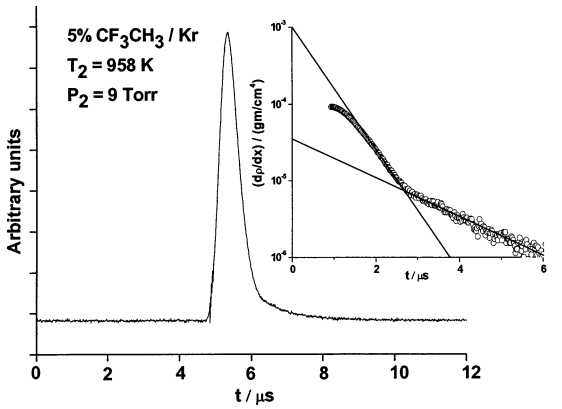

Figure 6. Vibrational relaxation of trifluoroethane in a second example showing double relaxation from a very low-P experiment whose temperature is again much too low for discernible dissociation. See caption in Figure 5.

Relaxation is extremely fast here as it is in all species with attached methyl groups.[29,30] However, as in several other such large molecules,[30] it can still be fully resolved at high temperatures for very low pressures. Examples of pure relaxation in CF_3CH_3 are presented in Figures 5 and 6, where the process is clearly seen to occur in two distinct stages. In other words, this is a double relaxation. Note that there is no possibility of dissociation being involved at these temperatures, where even the high-pressure literature rates of Figure 4 would predict an undetectably small gradient of $<10^{-11}$ gm/cm^4 (1000 K).

Double relaxation is a rare event, but has been seen in ultrasonic experiments at room temperature for a few molecules.[29] It seems it has not been observed before in trifluoroethane simply because relaxation in this molecule has not been studied. The one thing that such double relaxation unambiguously demonstrates is the presence of slow IVR. If intramolecular relaxation is fast relative to all T, R-V processes, the vibrational energy must relax as a unit, and only one relaxation time will then be seen.

Two relaxation times can be estimated from each experiment like those of Figures 5 and 6 by the usual methods.[18,30] Unfortunately these usual methods, which involve making corrections for the (variable) density ratio across the shock, ρ_2/ρ_1, i.e., the ratio of lab to molecule time, and introducing the Blythe-Blackman corrections[18] that convert density gradient times to Bethe-Teller[29] or energy relaxation times, cannot be strictly correct for the faster of the two processes seen here. In such fast relaxation we have routinely estimated all the needed quantities at vibrational equilibrium because it cannot be seen until close to equilibrium.[10,11,18,30] Temperatures and pressures given in Figures 5, 6, and 8 are so evaluated. This may well be a reasonable approximation for a single fast relaxation, but here the first process clearly does not end on complete equilibrium, so we do not know the conditions where it stops. Fortunately, the corrections either vary but little, i.e., the velocity ratio, or are small, the Blythe-Blackman correction, which is no more than 25%. The effect of this inapplicability is probably minor, introducing an error less than the scatter in the data for $P\tau_1$ (here $P\tau_1$ refers to the fast process, and $P\tau_2$ the slow) but its imperfection must be recognized.

Bethe-Teller energy-relaxation times[29] for both stages of the double relaxation are summarized in Figure 7 in the usual Landau−Teller plot of these second-order times scaled to one atmosphere pressure. There is no reason to believe that such fast relaxation will conform to the Landau−Teller temperature dependence, and in general it does not,[10,11,18,30] but no other

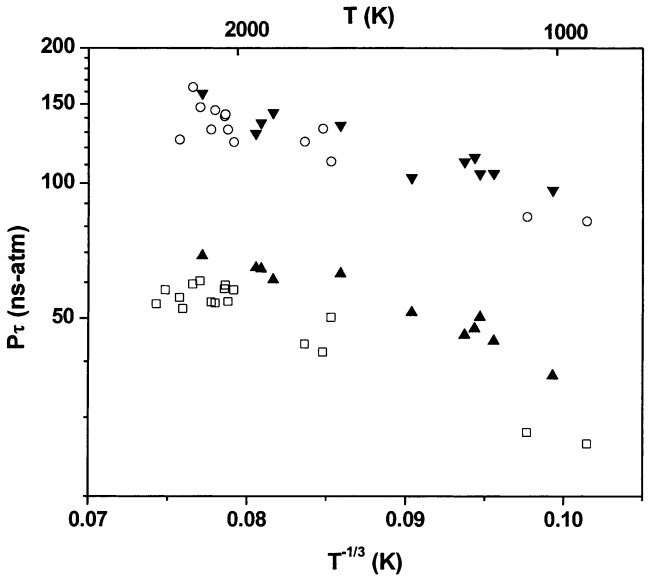

Figure 7. Landau-Teller plot of both vibrational relaxation times for 5% CH_3CF_3−Kr: [□], $P\tau_1$, 7−15 Torr; [▲], $P\tau_1$, 20−30 Torr; [○], $P\tau_2$, 7−15 Torr; [▼], $P\tau_2$, 20−30 Torr.

choice has been established. The best test for consistency in thermal relaxation is to compare relaxation times for different pressures. Referring to the figure, the two pressure groups (identified by filled and open symbols) can be seen to agree fairly closely, although the very short $P\tau_1$ values are a bit larger at the higher pressures. However, for these this extremely fast process is not as well resolved and the lower pressure data are probably more reliable. This is a difficult experiment. The motivation for doing the high-pressure experiments was mainly to obtain better accuracy in the slow process, where agreement seems close enough. Finally, no attempt was made to determine relative collision efficiencies for the two colliders, Kr and the CF_3CH_3, by varying mole fractions. Our previous experience in the relaxation of methyl hydrocarbons[30] shows this to be a difficult and probably useless effort when the relaxation is this fast. In any case, recognizing how efficient it is here, where the fast process must have a collision efficiency/transition probability very close to unity, any collision-partner specificity is rather unlikely.

Another calculation commonly used in the analysis of LS relaxation experiments is an integration of the gradients to a net density change, which can then be compared with calculated thermodynamic density changes from initial frozen relaxation conditions to complete equilibrium.[18,30] For an exponential gradient we have: $\rho_e - \rho_o = u_1\tau(d\rho/dx)_{t=0}$. We have not performed this calculation on the relaxation in trifluoroethane because it is very difficult and there are ambiguities in interpretation. When the relaxation is truly rapid as it is here, the extrapolation of the steep exponential gradient to $(d\rho/dx)_{t=0}$ becomes too sensitive to errors in the location of the time origin, $t = 0$. Here the faster process is comparable in speed to what was barely perceived in propane[30] where relaxation occurs in 1 or 2 collisions at room temperature,[29] and this integration did not turn out well. Also, the procedure is now ambiguous because it is not clear just at what time, or better, at what vibrational energy, the slower process is actually initiated (see below).

For the highest temperatures included in Figure 7, the process is complicated by subsequent dissociation. An example of this is presented in Figure 8, where we identify three stages: a very fast initial relaxation, a slower relaxation and, finally, a smaller tailing gradient from dissociation. Obviously, it is not a trivial

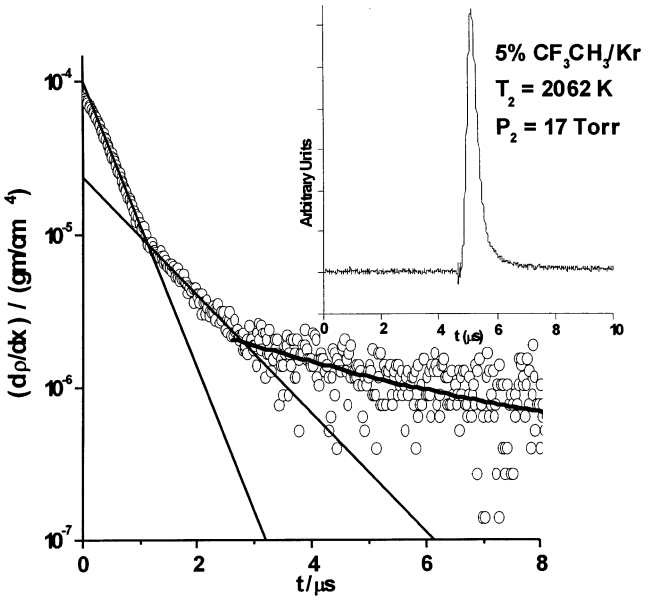

Figure 8. Example LS gradient profile (○) of a high-temperature shock wave in which both relaxation stages are resolved and where these are now followed by a clearly separate dissociation gradient. The inset shows the raw signal. Here the larger, semilog plot shows gradients with linear fits of the two relaxations and a kinetic-model fit of the dissociation. This calculation begins after the relaxation, i.e., following an incubation delay.

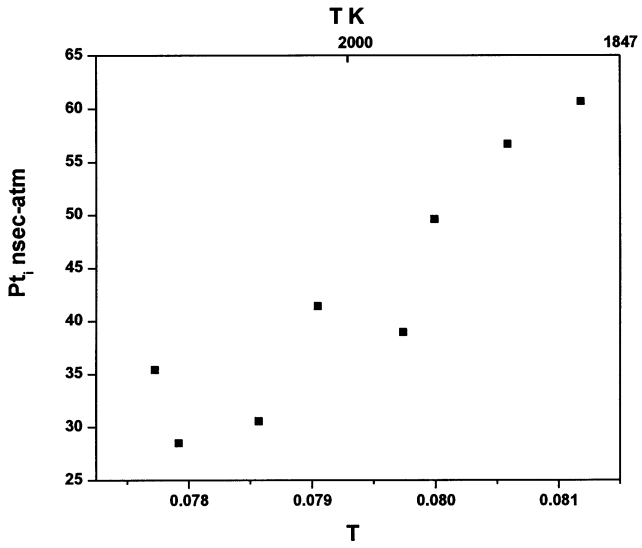

Figure 9. Incubation times for reaction (A) estimated from the length of the relaxation zone in experiments that exhibit all three processes as in the example of Figure 8.

matter to extract three separate rates from a single gradient profile, and the extraction shown here is unlikely to be very quantitative, but the experiment clearly allows such interpretation, so the data from several such experiments have been included in Figure 7. In Figure 8, for the last stage, dissociation, the line shows a calculated model gradient with a rate of reaction (A) chosen to fit the data. The modeling starts after completion of the entire relaxation, i.e., after a dissociation incubation delay. This process is presumed to begin at the end of the relaxation, i.e., the dissociation is delayed by an incubation time during which the total vibrational energy reaches a steady state.[31]

Experiments such as that shown in Figure 8 can be also used for an estimate of dissociation rate at extremely low pressures. Some rate constants derived from such a modeling have been included in the Arrhenius plot of Figure 3. They do seem to be consistent with the rest of the data but should be regarded as too uncertain for quantitative comparison with theory.

Incubation times (t_i) are also obtained from this analysis and these are shown in Figure 9. Here we do not follow the usual procedure of plotting t_i/τ because of the ambiguity caused by having two relaxation times. The resulting times are very short, as might be expected with such fast relaxation. Because they are so short, we may anticipate that they are probably more inaccurate than usual,[10,11,18] although recent work on such fast processes suggests that the time-origin error may actually be quite small for these conditions.[30] The incubation times introduced into the modeling of the low-pressure experiments of Figure 2 were obtained by scaling the data of Figure 9 to the higher pressures of these experiments assuming the usual second-order pressure dependence.

Analysis

Relaxation. The relaxation times of Figure 7 hardly uncover all aspects of the relaxation mechanism in trifluoroethane, but they do offer some hints. First, the temperature dependence and relative magnitudes of the relaxation times in Figure 7 offer a qualitative indication of the vibrational energy actually transferred in the two separate stages. That is, as noted before,[10,11,30] where relaxation is extremely efficient, i.e., either P_{10}[29] is near unity or $\langle\Delta E\rangle_{\text{down}}$ is nearly the size of the lowest vibration quantum, neither can much increase with T, and the process then appears to slow with increasing temperature simply because a strongly increasing amount of energy must be provided. Of course, this is what makes resolution possible in these experiments. Thus the larger $P\tau_2$ values for the slower stage suggest that this portion carries the greater part of the vibrational energy, and this observation helps lead to the interpretation of the observed falloff offered in the following paragraph.

We tentatively propose that this double relaxation is but another example of the classic "series" process,[29] but here one with slow IVR. The fast stage is probably collisional activation of the lowest mode, the torsion at 249 cm^{-1}, and the slow stage is then mainly IVR transfer from this mode to the remaining vibrations of the molecule. This mechanism entails the notion that direct collisional transfer to these latter modes is relatively slow, and this is entirely consistent with their higher frequencies (Table 1). A strong inverse correlation between vibration frequency and T, R-V transfer rate is well documented.[29] Also, the delay in this transfer indicated by the rather sharp separation of the two stages would seem to imply that a certain level of excitation in the torsion must be reached before IVR transfer occurs. Thus the duration of the first relaxation stage covers a kind of incubation delay for the second stage. These ideas are very similar to some proposed by Holmes et al.[32] to explain the double relaxation they saw in ethane.

Dissociation. The presence of the double relaxation and its above tentative interpretation suggests a division of the internal states of trifluoroethane into two sets, slowly communicating by intramolecular processes, with collisional excitation of just one portion and dissociation from the other. This notion can be used to construct a simple non-RRKM model of the dissociation that offers an estimate of the IVR rate necessary to match the experimental falloff. Such a simple separation has been used before in the theoretical treatment of non-RRKM reaction by Bunker and Hase,[1] who offer a charming diagram of the phase space, by Snider[33] as part of a more complex model, and by Marcus et al.,[34] in a consideration of chemical activation. Nonetheless, perhaps the only real justification for this approach

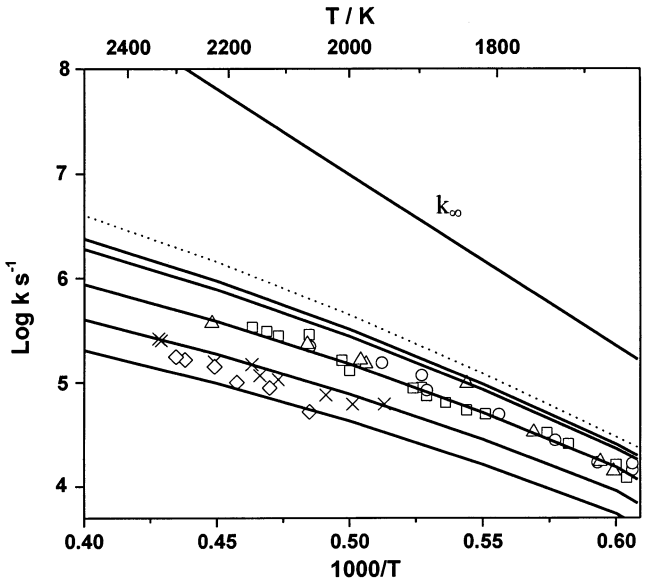

Figure 10. Comparison of a slow-IVR model RRKM calculation (see text) to the rate constants for reaction (A). This model is described in the text and in Table 1. Here the data are the same as in Figure 3 and the various pressures are denoted similarly. As before, the various calculations are for the specified mean pressures in this figure and are in ascending order of pressure. The dotted line is the "false limit" rate constant [1], described in the text. Again the heavy upper line displays the "true" k_∞ from the TST/G3 calculation described in the text.

is that it reduces the IVR-caused falloff to one parameter, which may then be estimated from a fit to the dissociation data. It would be difficult to extract much more than this.

We add a slow IVR step, here reaction 2, to an otherwise routine microcanonical Lindemann scheme, as

$$\mathrm{M} + \mathrm{A} \underset{k_{-1}}{\overset{k_1}{\rightleftharpoons}} \mathrm{A}^*(E) + \mathrm{M} \qquad (1)$$

$$\mathrm{A}^*(E) \underset{k_{-2}}{\overset{k_2}{\rightleftharpoons}} \mathrm{B}^*(E) \qquad (2)$$

$$\mathrm{B}^*(E) \xrightarrow{k_3} \text{products} \qquad (3)$$

Again, the state space is divided into two parts (here A, B), with reaction only from B*(*E*) and direct collisional excitation only of A to A*(*E*). We introduce a steady state on A*(*E*) and B*(*E*), and include the usual RRKM rates with parameters exactly as they are presented in Table 1, and as they were used in the earlier calculations. We choose $k_2/k_{-2} = 1$ (necessary for normal Lindemann behavior at low *T* where step (3) is slow) and we then have k_{uni} as the usual RRKM integral with k_{-1} (= $\beta_c Z_c(\mathrm{M})$, with $Z_c(\mathrm{M})$ the collision frequency) replaced by $k_{-1}k_2/(k_{-1} + k_2)$.

We have introduced the above IVR rate constant k_2 to our original RRKM program as indicated and run several calculations. The best of these is compared to the data in Figure 10, where the fit is seen to be much improved with an IVR rate constant, $k_2 \sim 10^8$/s. This is at the slow end of the scale of measured rates,[12] but it is certainly necessary for it to be this slow if it is to be rate controlling when k_∞, the average of $k(E)$, is of this size or smaller.

The last calculation also offers an estimate of the "false limit" rate constant[1] for this dissociation, i.e., the high-pressure limiting rate with slow first-order IVR, and this is included in Figure 10. As shown therein, nearly all the falloff under these conditions is IVR falloff; pressure or collisional falloff is minor. This is certainly consistent with the weak variation of the measured rates with pressure.

An important constraint that must be satisfied by the false limit rate is that it not destroy agreement with the earlier low-*T* data of Figure 4. At the highest temperatures reached in the Tschiukow-Roux et al.[25] study, 1310 K, the false limit rate is below the previous k_∞ by only some 14%, a drop that is barely discernible in the figure.

Also related to the false limit, a most interesting observation concerns the shock-tube results of Cadman et al.[26] who explored higher temperatures than the other literature work (1590−1865 K), and whose rates lie almost an order of magnitude below an extrapolation of this work and our k_∞ (see Figure 4). However, when the present model including IVR falloff is used for their conditions, the agreement is really much improved; they now differ from the model by a maximum of 70%. Here the result is strongly reduced by IVR falloff alone; pressure falloff is negligible for their above-atmospheric pressures.

Finally, at sufficiently high pressures the false limit must be overcome and the rate approach the true k_∞. This will occur with the above Lindemann scheme if one allows for direct collisional activation of the B*(*E*). This scheme is certainly much simplified and there are obviously many other complications that could exist in this system; for example, the IVR process might be partially promoted by collisions.

There are somewhat conflicting results concerning the applicability of RRKM theory to chemical activation experiments that result in HF elimination from CF_3CH_3. Parks et al.[35] formed CH_3CF_2 ^{18}F by hot ^{18}F displacement, and concluded that its decomposition is nonrandom because they found only HF, and no radical products, even for their highest energies, whereas Chang and co-workers[36] found RRKM to be a good fit to the chemically activated HF elimination when the CF_3CH_3 is formed by combination of $\bullet CH_3$ and $\bullet CF_3$. At room temperature this step leaves CF_3CH_3 with about 30 kcal/mol of excess energy above the HF loss threshold. RRKM may appear to be successful here simply because the rate is not large enough at this energy for slow IVR to interfere. It also might be a consequence of the location of the initial activation in the CC stretch. This is one of what we would probably identify as the accessible, reactive modes, i.e., part of B*, and direct excitation of this would then show little if any falloff caused by slow IVR into the reaction coordinate.

Conclusions

High-temperature, 1600−2300 K and fast dissociation, $k = 10^4-10^5$/s, in the dissociation of 1,1,1-trifluoroethane, appear to produce a strongly non-RRKM dissociation reaction. TST rates for k_∞, taken from electronic-structure calculations, although in superb agreement with previous low-*T* data, are orders-of-magnitude higher than the present measurements when extrapolated to these temperatures. Nonetheless, this severe falloff is not reflected in a significant pressure dependence of the measured rates. This inconsistency leads to a serious and seemingly irreparable failure of RRKM models of the process. This reaction thus appears to be a quite unambiguous intrinsic non-RRKM dissociation. There are other possible causes for an apparent failure of RRKM theory; for one thing, the theory used might be seriously inadequate because it does not recognize some very large anharmonic effects in the molecular state density. This seems even more unlikely than the current notion of non-RRKM reaction, but such complications are not impossible.

A severe falloff without much pressure dependence implies that first-order steps, i.e., intramolecular processes, or collision-

free IVR, have become rate-limiting. Such IVR falloff can be introduced to a microcanonical Lindemann scheme through a simple division of the activated molecule states into two groups communicating by slow IVR. When this is implimented, the collisional term in the RRKM rate expression, here the deactivation rate constant, $\beta_c Z_c(M)$, is simply replaced by $\beta_c Z_c(M) k_{IVR}/(\beta_c Z_c(M) + k_{IVR})$, where the added term is the IVR rate connecting the two groups of states. Modeling of the data with this modification of RRKM is reasonably successful with $k_{IVR} \sim 10^8$/s. Measurements of vibrational relaxation, resolvable at very low pressures, show a two- stage process, a double relaxation, and thus unambiguous evidence of slow IVR, at least at low energies. Here the tentative suggestion is that this process involves prior excitation of the low-frequency torsion which then IVR transfers to the remaining modes of the molecule.

Finally, we offer the possibly useful notion that double relaxation may well be necessary (but not sufficient) for non-RRKM dissociation. If one cannot find slow IVR at the bottom of the ladder of states, why would it occur at the high energies involved in dissociation? Thus double relaxation may well be a strong and relatively accessible indicator of non-RRKM behavior. Certainly it helps explain why the phenomenon is so rare; despite numerous studies of molecules in relaxation[29] very few double processes have been uncovered.

Acknowledgment. We thank D. C. Fang and L. B. Harding for the G3 calculations of the transition state for the trifluoroethane dissociation. This research was supported by the U.S. Department of Energy, Division of Chemical Sciences, under Grant No. DE-FE−85ER13384 and this support is gratefully acknowledged.

References and Notes

(1) Bunker, D. L.; Hase, W. L. *J. Chem. Phys.* **1973**, *59*, 4621. Bunker, D. L. *The Theory of Elementary Reaction Rates*; Pergamon: London, 1966.

(2) Holbrook, K. A.; Pilling, M. J.; Robertson, S. H. *Unimolecular Reactions*; Wiley: New York, 1996. Pritchard, H. O. *The Quantum Theory of Unimolecular Reactions*; Cambridge: London, 1984. Forst, W. *Theory of Unimolecular Reactions*; Academic Press: New York, 1973. Gilbert, R. G.; Smith, S. C. *Theory of Unimolecular and Recombination Reactions*; Blackwell: Oxford, 1990.

(3) Some examples, among many, are: Wilson, D. J. *J. Phys. Chem.* **1960**, *64*, 323. Grant, E. R.; Bunker, D. L. *J. Chem. Phys.* **1978**, *68*, 628. Hedges, R. M.; Reinhardt, W. P. *Chem. Phys. Lett.* **1982**, *91*, 241. Hase, W. L.; Wolf, R. J. *J. Chem. Phys.* **1981**, *75*, 3809. Hase, W. L.; Wolf, R. J.; Sloane, C. S. *J. Chem. Phys.* **1979**, *71*, 2911. Schofield, S. A.; Wolynes, P. G. *Chem. Phys. Lett.* **1994**, *217*, 497. Shalashilin, D. V.; Thompson, D. L. *J. Chem. Phys.* **1997**, *107*, 6204.

(4) Meagher, J.; Chao, K. J.; Barker, J. R.; Rabinovitch, B. S. *J. Phys. Chem.* **1974**, *78*, 2535.

(5) Rodgers, P. J.; Selco, J. I.; Rowland, F. S. *Chem. Phys. Lett.* **1983**, *97*, 313.

(6) See Meyer, A.; Schroeder, J.; Troe, J.; Votsmeier, M. *J. Phys. Chem.* **2001**, *105*, 4381, and references therein.

(7) Kappel, Ch.; Luther, K.; Troe, J. *Phys. Chem. Chem. Phys.* **2002**, *4*, 4392.

(8) Klippenstein, S. J.; Harding, L. B. *J. Phys. Chem.* **1999**, *103*, 9388.

(9) Kiefer, J. H. *Proc. Combust. Inst.* **1998**, *27*, 113.

(10) Srinivasan, N. K.; Kiefer, J. H.; Tranter, R. S. *J. Phys. Chem.* **2003**, *107*, 1532.

(11) Santhanam, S.; Kiefer, J. H.; Tranter, R. S.; Srinivasan, N. K. *Int. J. Chem. Kinet.* **2003**, *35*, 381.

(12) Lehmann, K. K.; Scoles, G.; Pate, B. H. *Annu. Rev. Phys. Chem.* **1994**, *45*, 241.

(13) Fletcher, F. J.; Rabinovitch, B. S.; Watkins, K. W.; Locker, D. J. *J. Phys. Chem.* **1966**, *70*, 2823, and references therein.

(14) Collister, J. L.; Pritchard, H. O. *Can. J. Chem.* **1976**, *54*, 2380.

(15) Dianxun, W.; Ximei, Q.; Peng, J. *Chem. Phys. Lett.* **1996**, *258*, 149.

(16) Kiefer, J. H.; Manson, A. C. *Rev. Sci. Instrum.* **1981**, *52*, 1392.

(17) Kiefer, J. H., In *Shock Waves in Chemistry*; Lifshitz, A., Ed.; Marcel Dekker: New York, 1981; p 219.

(18) Kiefer, J. H.; Kumaran, S. S.; Sundaram, S. *J. Chem. Phys.* **1993**, *99*, 3531. See also ref 10 and ref 11.

(19) Gardiner, W. C., Jr.; Hidaka, Y.; Tanzawa, T. *Combust. Flame* **1981**, *40*, 213.

(20) Stein, S. E.; Ruckers, J. M.; Brown, R. L. *NIST Stand. Ref. Database* 25, *Thermochemical Data, version* 1.2, 1991.

(21) NIST Computational Chemistry Comparison and Benchmark Database, *NIST Stand. Ref. Database*, http://kinetics.nist.gov/index.php 2003, 101.

(22) Just, Th. *Proc. Combust. Inst.* **1994**, *25*, 687.

(23) Curtiss, L. A.; Ragavachari, K.; Redfern, P. C.; Rassolov, V.; Pople, J. A. *J. Chem. Phys.* **1998**, *109*, 7764.

(24) Sianesi, D.; Nelli, G.; Fontanelli, R. *Chimica e L'Industria* **1968**, *50*, 619.

(25) Tschiukow-Roux, E.; Quiring, W. J. *J. Phys. Chem.* **1971**, *75*, 295.

(26) Cadman, P.; Day, M.; Trotman-Dickenson, A. F. *J. Chem. Soc. A* **1971**, 1356.

(27) Tsang, W.; Lifshitz, A. *Int. J. Chem. Kinet.* **1998**, *30*, 621.

(28) Mitin, P. V.; Barabanov, V. G.; Volkov, G. V. *Kinet. Catal.* **1988**, *29*, 1279.

(29) Cottrell, T. L.; McCoubrey, J. C. *Molecular Energy Transfer in Gases*; Butterworths: London, 1961. Stevens, B. *Collision Activation in Gases*; Pergamon: London, 1967. Lambert, J. D.; Salter, R. *Proc. Roy. Soc.* **1959**, *A253*, 277.

(30) Kiefer, J. H.; Sahukar, G. C.; Santhanam, S.; Srinivasan, N. K.; Tranter, R. S. *J. Chem. Phys.* **2004**, *120*, 918.

(31) See Tsang, W.; Kiefer, J. H. Unimolecular Reactions of Large Polyatomic Molecules. *Advanced Series in Physical Chemistry, Chemical Dynamics and Kinetics of Small Radicals Pt. 1*; World Scientific: Singapore, 1995; p 58. Also note refs 10, 11, and 18.

(32) Holmes, R.; Jones, G. R.; Pusat, N. *J. Chem. Phys.* **1964**, *41*, 2512.

(33) Snider, N. *J. Phys. Chem.* **1989**, *93*, 5789.

(34) Marcus, R. A.; Hase, W. L.; Swamy, K. N. *J. Phys. Chem.* **1984**, *88*, 6717.

(35) Parks, N. J.; Krohn, K. A.; Root, J. W. *J. Chem. Phys.* **1971**, *55*, 5785.

(36) Chang, H. W.; Craig, N. L.; Setser, D. W. *J. Phys. Chem.* **1972**, *76*, 954.

(37) Gilbert, R. G.; Luther, K.; Troe, J. *Ber. Bunsen-Ges. Phys. Chem.* **1983**, *87*, 169.

(38) Pitzer, K. S.; Gwinn, W. D. *J. Chem. Phys.* **1942**, *10*, 428.

(39) Troe, J. *J. Phys. Chem.* **1979**, *83*, 114.

(40) Troe, J. *J. Chem. Phys.* **1977**, *66*, 4758.